Information Theory Based Fingerprint Matching

Lifeng Liu, Jianwei Yang, Chaozhe Zhu and Tianzi Jiang*, *Member, IEEE*

National Laboratory of Pattern Recognition, Institute of Automation,
Chinese Academy of Sciences, Beijing 100080, P. R. China.
Email: {lfliu, jwyang, czzhu, jiangtz}@nlpr.ia.ac.cn

Running Title: Information Theory Based Fingerprint Matching

*Correspondence Address:

Tianzi Jiang
National Laboratory of Pattern Recognition
Institute of Automation,
Chinese Academy of Sciences
Beijing 100080, P.R. China
Phone: +86 10 8261 4469
Fax: +86 10 6255 1993
Email: jiangtz@nlpr.ia.ac.cn

Abstract

Fingerprint matching is a critical step in fingerprint verification. Although a variety of algorithms have been proposed for this issue, accurate fingerprint registration is still an unresolved problem. This paper proposes a novel fingerprint registration method, which is based on information theory. This algorithm finds the accurate alignment by maximization of mutual information between features extracted from orientation fields of template and input fingerprint images. The primary characteristic of this method is that it uses global feature (orientation field) to align fingerprints and its behavior resembles what human acts when comparing fingerprints. Experimental results show that the occurrences of misalignment can be dramatically reduced. Meanwhile, registration accuracy is greatly improved, which will undoubtedly enhance matching performance. In minutiae matching, a fuzzy approach to the computation of matching scores is designed to better reflect the fineness of matching. Good verification performance of this method has been achieved on a fingerprint database.

Index Terms: Biometrics, fingerprints, information theory, mutual information, minutia, orientation field, registration, matching.

1 Introduction

Fingerprints are flow-like ridges being present on human fingers. Fingerprint-based personal identification has been used for a very long time [13]. Owning to their uniqueness and immutability, fingerprints today have been the most widely used biometric features. Nowadays, most automatic fingerprint identification systems (AFIS) are based on minutiae matching. Minutiae are local ridge characteristics in the fingerprint pattern. The two most prominent minutiae are ridge ending and ridge bifurcation (see Fig. 1).

Generally, fingerprint matching can be roughly classified into four categories, namely image-based, graph-based, filterbank-based and minutiae-based. The image-based matching [1] uses the entire gray scale fingerprint image as template to match against input fingerprint images. The primary shortcoming of this method is that matching may be seriously affected by some factors like contrast variation, image quality variation and distortion which are inherent properties of fingerprint images. Such limitations result from that gray scale values of a fingerprint image is not a stable feature, which may change from different impressions. Another drawback is the large size of template since the whole gray scale image is to be stored. In addition, in some countries, it is illegal to store entire fingerprint due to the possibility of invasion of privacy. Another approach, i.e., matching by entire ridge structure, which is inherently image-based, is invariant to the brightness variations but is very sensitive to image quality. Graph-based matching [4] [6] represents minutiae in the form of graphs. The high computational complexity of graph matching hinders its implementation.

A.K. Jain [10] proposed an innovative approach to vie with the classical minutiae-based matching algorithms. This method first detects a reference point and then tessellates the fingerprint around this point. Afterwards, a bank of Gabor filters (oriented in eight directions) is used to construct a feature vector named FingerCode. Thus, matching between two fingerprint images reduces to finding the Euclidean distance between two FingerCodes. The salient advantage of this method is that it will be very efficient to match a query fingerprint against a very large database because it uses index/retrieval mechanism. However, it is impossible to locate the reference point precisely each time and at some times it even cannot be detected at all due to poor image quality or only partial finger present in the image, which is fatal to the method. Furthermore, it is sensitive to deformation as claimed in the paper. All of these shortcomings limit the application of this method for reliable identification.

Minutiae-based matching matches two sets of minutiae of template and input fingerprint images to determine whether the two fingerprint images are from the same finger. This can be done with point pattern matching. Several point pattern matching algorithms have been proposed in the literature [15][18][20]. Some comments on them were made [7][8]. The point pattern matching is generally intractable due to the lack of knowledge about the correspondence between two point sets. To address this problem, A.K. Jain proposed alignment-based minutiae matching algorithms [7][8]. The two sets of minutiae are first aligned using corresponding ridges to find a reference minutiae pair, one from the input fingerprint and another from the template fingerprint, and then all the other minutiae of both images are converted with respect to reference minutiae. Afterwards, the aligned point patterns are matched to give a matching result. X. Jiang [11] proposed an improved method, which uses minutia together with its neighbors to find the best registration. All of these approaches may fail when the correct alignment cannot be recovered, which often happens when applied to poor quality fingerprint images.

This paper proposes a novel fingerprint matching algorithm, in which the best alignment of two fingerprint images, template and input, is achieved by maximization of mutual information between features extracted from their orientation fields and the matching result is jointly given by minutiae matching and the resulted mutual information achieved during registration. Orientation field of a fingerprint image, which is a stable feature independent of fingerprint capture devices and contrast variation, represents the intrinsic nature of a fingerprint image and can generally be estimated reliably. While comparing two fingerprints, we first use the global structure (orientation field) to find the correspondence of two fingerprints and then use local characteristics (minutiae) to give a matching result. Our method much resembles what human behaves and is easy to implement. For minutiae matching, we integrated the registration result into the final decision and propose a fuzzy approach to the computation of matching scores. Experimental results show that our algorithm achieves accurate registration and excellent verification performance.

The rest of this paper is organized as follows. Section 2 gives the definitions of entropy and mutual information. In section 3, our feature extraction method is briefly described. Section 4 devotes to information theory based matching algorithm. Experimental results on a fingerprint database are described in Section 5. The summary and discussion are outlined in Section 6.

2 Entropy and Mutual Information

2.1 Entropy

Entropy is a statistical measurement that summarizes randomness. Given a discrete random variable X, its entropy is defined by

$$H(X) = -E_X[\log P(X)] = -\underset{x_i ? \Omega_x}{?} P(X = x_i)\log P(X = x_i) \tag{1}$$

where Ω_x is the sample space and x_i is the member of it. $P(X = x_i)$ represents the probability when X takes on the value x_i. We can see in equation (1) that the more random a variable is, the more entropy it will have.

2.2 Conditional Entropy, Joint Entropy and Mutual Information

Conditional and joint entropy relates the predictability of two random variables'. Conditional entropy and joint entropy are defined as follows:

$$H(Y \mid X) = -E_X[E_Y[\log P(Y \mid X)]] = -\underset{x_i ? \Omega_x}{?}\ \underset{y_j ? \Omega_y}{?} P(X = x_i, Y = y_j) \log P(Y = y_j \mid X = x_i) \tag{2}$$

$$H(XY) = E_X[E_Y[\log P(Y, X)]] = -\underset{x_i ? \Omega_x}{?}\ \underset{y_j ? \Omega_y}{?} P(X = x_i, Y = y_j) \log P(Y = y_j, X = x_i) \tag{3}$$

Conditional entropy measures the randomness of Y when X is given and joint entropy measures the randomness of Y and X. With the increase of $H(Y \mid X)$, Y gets more dependent on X. However, conditional entropy by itself is not a measure of dependency. A small value of $H(Y \mid X)$ implies either $H(X)$ is small or Y is less dependent on X.

When Y and X are independent, (2) and (3) can be expressed using $H(X)$ and $H(Y)$:

$$H(Y \mid X) = H(Y) \tag{5}$$

$$H(XY) = H(X) + H(Y) \tag{6}$$

Mutual information, MI, between two random variables is defined as:

$$I(Y, X) = H(Y) - H(Y \mid X) \tag{7}$$

Because conditional entropy can be expressed in terms of marginal and joint entropies:

$$H(Y \mid X) = H(XY) - H(X) \tag{8}$$

We can get two equivalent expressions for MI:

$$I(X, Y) = H(X) - H(X \mid Y) \tag{9}$$

$$I(X, Y) = H(X) + H(Y) - H(XY) \tag{10}$$

MI measures the statistical dependency between two random variables. The physical meaning of MI is the reduction in entropy of Y given X.

P. Viola [21] proposed that registration could be achieved by maximization of mutual information. In this paper, we apply mutual information in fingerprint registration and matching. The details will be described in Section 4.

3 Feature Extraction

In feature extraction, we want to extract orientation field and minutiae, i.e. endpoints and bifurcations, of both template and input fingerprint images. Orientation field is a reliable feature of fingerprint images, which is very important for fingerprint enhancement, minutiae extraction and matching. Minutia is another stable feature which most matching algorithms are based on.

3.1 Orientation Field Estimation

Fingerprint images can be regarded as an oriented texture pattern. The orientation field of a fingerprint image, which is a stable feature independent of fingerprint capture devices, represents the intrinsic nature of the fingerprint image. In our algorithm, orientation field plays a crucial role in aligning two fingerprint images, template and input, and fingerprint enhancement as well.

A.R. Rao [16] proposed an algorithm to estimate the orientation of texture images. The orientation field is used to compute the optimal dominant ridge direction in each $16?16$ window or block. Rao's algorithm consists of the following main steps [16]:

1) Divide the input fingerprint image into blocks of size $16?16$.

2) Compute the gradients G_x and G_y at each pixel in each block.

3) Estimate the local orientation of each block using the following equation:

$$\theta(i,j)=\frac{1}{2}\tan^{-1}\begin{matrix}?\\?\\?\\?\\?\\?\end{matrix}\frac{\overset{i+8}{\underset{u=i-8}{?}}\ \overset{j+8}{\underset{v=j-8}{?}}\ 2G_x(u,v)G_y(u,v)}{\overset{i+8}{\underset{u=i-8}{?}}\ \overset{j+8}{\underset{v=j-8}{?}}\ (G_x^2(u,v)-G_y^2(u,v))}\begin{matrix}?\\?\\?\\?\\?\\?\end{matrix} \qquad (11)$$

Where G_x and G_y are the gradient magnitudes in x and y directions, respectively. Finally $\theta(i,j)$ is regularized into the range of $-90^\circ \sim 90^\circ$.

A.K. Jain [7] proposed a hierarchy approach to estimate the orientation more precisely. In this paper, we do not use this hierarchy approach because the inexactness will affect our algorithm very little. That is, we average all the pixels' direction within a window to get a mean direction. So Rao's algorithm is more efficient here. In order to further speed up the process of the orientation field computation, we use a sliding window to efficiently calculate every pixel's direction in the entire fingerprint image.

After the orientation field is estimated, direction features can be calculated. During fingerprint template enrollment, we divide the whole fingerprint image into $W ? W$ blocks and the mean of directions in each block is computed. In this step, the marginal blocks are excluded because in our tested database the fingerprint region does not take up the entire image. Thus, the directions of marginal blocks are meaningless. All the directions of computed blocks are stored as features for registration and matching described later. Fig. 2 shows a fingerprint and its mean directions in different blocks.

3.2 Minutia Detection

Minutia detection intends to locate minutiae and record their attributes including coordinates, directions, and types. This section briefly described our method to detect minutiae.

3.2.1 Topographic Segmentation of Fingerprint Images

Before the topographic segmentation is carried out, region of interest of fingerprint images is located based on the local variance of gray level. In doing so, we assume that there is only one fingerprint present in the image.

Topographic segmentation of fingerprint images [19] is based on the topographic property of the image surface, which is treated as a noisy sampling of the underlying continuous surface approximated by orthogonal Chebyshev polynomials. Ridge and valley are discriminated by the sign of the maximum normal curvature of the continuous surface.

This method can connect short gaps and eliminate blemishes along the ridge and valley lines, which dramatically enhanced the fingerprint. Another advantage is that the resulting image is already binary and no binarization is required afterwards.

3.2.2 Thinning and Minutia Detection

Prior to thinning, we use morphological closing to the segmented fingerprint to eliminate small holes and connect broken ridges. Then the binary image is thinned using algorithm in [2]. We assume that if a pixel is on a thinned ridge, then it has a value 1, and 0 otherwise. Thanks to the good result of segmentation, the thinned image is fairly smooth. Minutiae can be easily detected by counting the occurrences of 1 in its eight neighbors of a pixel located on a ridge.

3.2.3 Post-processing

There are usually over one hundred minutiae detected in the thinned binary fingerprint images, while there exist less than 60 minutiae in a real fingerprint. This arises as a consequence of wrinkle, scars and stains, etc. The existence of false minutiae will seriously influence the matching result so that post-processing is needed to eliminate most imposter minutiae and at the same time retain genuine ones. Post-processing used in our algorithm is similar to the one in [3].

4 Fingerprint Matching

The purpose of fingerprint matching is to determine whether two fingerprints, template and input, are from the same finger. To this end, we assume that minutiae and direction features of the template fingerprint image have been extracted during enrollment, and the minutiae and orientation field of the input fingerprint image have been extracted in the feature extraction stage. Now the matching between two fingerprint images changes to matching between two sets of minutiae and direction features. Since we do not have any prior knowledge about what the relative position of the two fingerprints, we must first align them to get the correct correspondence. Then matching between two sets of minutiae is carried out to get the matching result. Our method of matching can be divided into two stages, namely registration and matching.

4.1 Registration Using Mutual Information

Registration or alignment is the process by which the correct transformation is extracted. The definitions of entropy and mutual information, MI, are described in Section 2. Here we will use MI between template and input's direction features to align two fingerprints. Although MI can be estimated using equation (7), (9) or (10), the difficulty of estimating conditional entropy of two random variables hinders the application of both (7) and (9). Fortunately, we can estimate MI using (10) with some conversion of random variables.

In our registration algorithm, the distortion is not considered because the template and input fingerprint images are captured with the same device so that the distortion is not very large. Given a certain transformation $(\Delta x, \Delta y, \Delta\theta)$, the orientation field of the input fingerprint image can be transformed into the template coordinate system:

$$\begin{bmatrix} x' \\ y' \end{bmatrix} = \begin{bmatrix} \cos\Delta\theta & -\sin\Delta\theta \\ \sin\Delta\theta & \cos\Delta\theta \end{bmatrix} \begin{bmatrix} x \\ y \end{bmatrix} + \begin{bmatrix} \Delta x \\ \Delta y \end{bmatrix} \tag{12}$$

The transformed orientation field image is superposed on the imaginary template image (template image is not present in matching phase). The resulted image is divided into blocks in the same way as did for template image during enrollment. The mean direction θ of each overlapped blocks can be computed as did for template. To keep the reliability of the mean direction, we drop the blocks whose overlapped size is less than four-fifths of the whole block size (see Fig. 3). When the number of overlapped blocks is less than one-third of the entire direction blocks used in the template image, the transformation is discarded because a too small overlapped size usually means a false registration, and as a result some images from same fingers may not be aligned. This is reasonable because when overlapped area is small, there is no sufficient evidence to verify whether the two images are from the same finger or images from different fingers are accidentally aligned.

The mean direction θ ranges from $-90^\circ \sim 90^\circ$, inclusive. For convenience of expression, we convert it to $0^\circ \sim 180^\circ$, inclusive. In order to estimate MI, the continuous direction θ needs to be evenly discretized and the continuity between 0° and 180° should be reserved:

$$\begin{aligned} &\theta_0 = [180^\circ - \frac{\Delta\theta}{2}, 180^\circ]?\ [0^\circ, \frac{\Delta\theta}{2}] \\ &\theta_i = [i?\,\Delta\theta - \frac{\Delta\theta}{2}, i?\,\Delta\theta + \frac{\Delta\theta}{2}] \quad i = 1,\ldots,n-1; \\ &\Delta\theta = \frac{180^\circ}{n} \end{aligned} \tag{13}$$

where *n* is the number of discrete directions.

Having discretized both the template and transformed input mean directions, we can define joint probability of an overlapped block (see Fig. 4). For example, if the mean direction of the template of a certain block falls into the range of θ_i and the corresponding transformed input mean direction falls into the range of θ_j, then the element $n(i, j)$ of joint probability adds one. After all the overlapped blocks are examined, we can get the joint and marginal probability distributions using the following equations:

$$\begin{aligned} &P_{XY}(i, j) = \frac{n(i, j)}{\mathop{?}\limits_{i=0}^{n-1} \mathop{?}\limits_{j=0}^{n-1} n(i, j)} \\ &P_X(i) = \mathop{?}\limits_{j=0}^{n-1} P_{XY}(i, j) \\ &P_Y(j) = \mathop{?}\limits_{i=0}^{n-1} P_{XY}(i, j) \end{aligned} \tag{14}$$

then MI of a given transformation can be estimated using equation (1), (3) and (10).

We have put forward an approach to estimate MI between mean directions of template and input fingerprint images given a transformation. Now, we need to search the parameter space to find the maximal MI so that the best registration between two fingerprints can be obtained. Fig. 5 shows the searching space. Although the parameter space is not very large, in comparison to a 3-D rigid object registration with six parameters to be recovered, which makes it not necessary to use an optimization algorithm, it is still time-consuming to search the whole parameter space pixelwise (in our experiments the rotation, translation of *X* and *Y* are set as $-24^{\circ} \sim 24^{\circ}$, -90 ~ 90, -63 ~ 63, respectively). To resolve the contradiction between processing time and accuracy, we use a hierarchy approach: coarse and fine registration.

In coarse registration, we search the parameter space with a relatively large step (in our experiments, rotation, translation of *X* and *Y* are12°, 9 and 9, respectively) to find the maximal MI, which indicates an approximate alignment. It should be noticed that if the searching step is too large, the program may be trapped in local maximum and the best registration couldn't be found. Otherwise, if searching step is too small, the computation will be very heavy. So this is a trade-off between efficiency and accuracy. Then in fine registration, we find the best transformation in the sub space around the resulted parameters. The best transformation with maximal MI can usually be found using the above-mentioned strategy and the corresponding MI and transformation is recorded for matching described below.

4.2 Matching

In this section, we will judge whether two fingerprints are from the same finger or not based on maximal MI and minutiae matching. Since our registration result strongly resembles human's observation to fingerprints, we can define four categories of situation in real matching as a human compares fingerprints:

(i) From the same finger with high similarity (large MI);

(ii) From the same finger but with less similarity because of noise or small area of overlapped sections (medium MI);

(iii) From different fingers but with high similarity possibly because they belong to the same class (medium MI);

(iv) From different fingers with little similarity (small MI).

By thresholding MI, we can partially differentiate (i) and (iv) from (ii) and (iii). When MI is greater than a threshold T_s, we say the two fingerprints are from the same finger (i). And if MI is less than a threshold T_d, the two fingerprints are coming from different fingers (iv). The other two cases (ii) and (iii) cannot be differentiated solely from MI. So they have to be further studied.

In the last section, the transformation between template and input fingerprints is recovered. We use these parameters to transform input minutiae into the coordinate system of the template minutiae:

$$\begin{aligned} &\theta_i^{'} = \theta_i + \Delta\theta \\ &\begin{bmatrix} x_i^{'} \\ y_i^{'} \end{bmatrix} = \begin{bmatrix} \cos\Delta\theta & -\sin\Delta\theta \\ \sin\Delta\theta & \cos\Delta\theta \end{bmatrix} \begin{bmatrix} x_i \\ y_i \end{bmatrix} + \begin{bmatrix} \Delta x \\ \Delta y \end{bmatrix} \end{aligned} \tag{15}$$

Due to the same reasons stated in [7], we also match minutiae in the polar coordinate systems. We convert each of the template and input minutiae to the polar coordinate system with respect to the central point of template image:

$$\begin{bmatrix} r_i \\ \varphi_i \\ \theta_i \end{bmatrix} = \begin{bmatrix} \sqrt{(x_i^* - x^c)^2 + (y_i^* - y^c)^2} \\ \tan^{-1}\left(\dfrac{y_i^* - y^c}{x_i^* - x^c} \right) \\ \theta_i^* \end{bmatrix} \tag{16}$$

where $(x_i^*, y_i^*, \theta_i^*)$ are the coordinates of a minutia, and $(x^c, y^c, 0)$ are the coordinate of the central point of the fingerprint image, and $(r_i, \varphi_i, \theta_i)$ is the representation of the minutia in polar coordinate system.

Although the registration by maximizing MI can find fairly good pose transformation, the nonlinear deformation of fingerprints, an inherent property of fingerprint images that cannot be recovered, and inexact minutiae extraction make it impossible to locate the template minutia and corresponding input minutia at the same position. Therefore, the matching should be elastic by using a 3-D boundary box in the polar coordinate system instead of an exact matching. We use a changeable boundary box whose size is changed according to different radius due to the fact that when radius is large, a small change in radial angle may introduce a large shift in distance between minutiae. Furthermore, we use a fuzzy approach to reflect the similarity level between a template minutia and the corresponding input minutia fell into the boundary box around the template minutia instead of the simple “matched” or “unmatched” result. The similarity level of a given pair is given as follows:

$$sl_i = \frac{\overset{?}{\underset{?}{?}}(1-\frac{\Delta r}{r}) + (1-\frac{\Delta\varphi}{\varphi_r}) ? 2 + (1-\frac{\Delta\theta}{\theta}) ? 2\overset{?}{\underset{?}{?}}}{5} \qquad (17)$$

where $\Delta r, \Delta\varphi, \Delta\theta$ are the differences of radius, radial angle and minutiae directions between template and input minutia, respectively. r and φ_r are the maximal tolerant differences of radius and radial angle for a given radius and θ is the maximal minutia direction difference permitted. Because direction is more discriminative than radius, we use a weighted sum to emphasize the differences in directions. Thus, each pair of minutiae fell into the boundary box is assigned with a similarity level ranging from 0 to 1 to represent the fineness of matching.

After all the matched pairs are found and the associated similarity levels are computed, we average all the similarity levels to get an average similarity level. The final matching score for two fingerprints is given according to the following equation:

$$ms = \frac{MI}{Ts} ? \frac{m}{\sqrt{MN}} ? sl ? 100 \qquad (18)$$

where *MI* is mutual information estimated in the registration stage, T_s is threshold for MI as described above. *m*, *M* and *N* represents the number of matched pairs of minutiae and the number of minutiae for template and input fingerprints, respectively. And *sl* is the average similarity level. In this equation both the registration and minutiae matching results are considered. Two fingerprints will be verified as from the same finger if their matching score is higher than a threshold. Otherwise, they are considered to come from different fingers.

5 Experimental Results

We have tested our novel fingerprint matching algorithm on the database downloaded from Universit? di Bologna, Italy. This Database contains 168 fingerprint images from 21 different fingers with 8 images per finger. The size of these images is 256? 256. These fingerprints images vary in quality. Fig. 6 shows some of the fingerprint images. Each fingerprint image is matched against all the other ones in the database. So, a total of 28056 (168? 167) matching times have been performed.

5.1 Registration

In our experiments, the rotation, translation of *X* and *Y* are set as $-24 \sim 24^{\circ}$, -90 ~ 90, -63 ~ 63, respectively. The registration is decomposed into three levels. The size of *W*? *W* window used to compute mean direction is 8? 8. The number *n* of discretized mean direction is 9, 18 and 36. Every fingerprint image in the database is aligned with all the other 167 ones. So a total of 1176 (7? 8? 21) alignments from same fingers and 26880 (160? 168) alignments from different fingers are performed. Fig. 7 shows normalized distributions of MI for same and different fingers (*W*=8 and *n*=18). Table 1 lists the mean and standard deviation of MI distributions and the number of misalignment of same fingers for different parameters. The number of misalignment using minutiae matching which is similar to [17] is also listed in the same table. From this table we can see that our algorithm is superior to general minutiae-based registration in the reduction of false registrations. We also observed that when *n* is large, for example 36 in our experiments, the errors of misalignment dramatically increased and they are quite stable when *n* is smaller, 9 and 18 in our experiments. The reason for this phenomenon is that when *n* gets larger, the mean direction is discretized more accurately and much sensitive to orientation field. As a result a small change in mean direction may greatly affect its distribution. Thus, when *n* is large, registration is much more sensitive to image quality which may affect the estimation of orientation field. Generally, our proposed algorithm can align two fingerprint images more accurate than minutiae-based method. Fig. 8 shows some comparisons of registration results. In Fig. 9 an example of registration, which is similar to the registration by human, is demonstrated. From all these experimental results we can argue that the proposed algorithm is very robust and accurate.

5.2 Matching

In experiments for minutiae matching, we set the largest differences of radius, radial angle and minutiae direction at $13.0, \frac{\pi}{9}, \frac{\pi}{8}$, respectively and *W*=8 and *n*=18 in the registration phase. The tolerance box is varied linearly with respect to the radius of a minutia. T_s and T_d of MI as described in Section 4.2 is set as 2.0 and 1.2, respectively.

The normalized distributions of matching scores for same fingers and different fingers are shown in Fig. 10. In drawing this figure, we do not use MI to judge matching result in order to keep the consistency of matching scores. Table 2 shows the FRR (False Reject Rates) and FAR (False Accept Rates) with different threshold values, in which MI is incorporated. FRR is defined as the percentage of fingerprints from same fingers are rejected as from different ones and FAR is defined as the percentage of fingerprints from different fingers are accepted as from the same one. We observed that matching errors are caused mainly by inexact minutiae detection, which are seriously affected by image quality. We can improve this by excluding poor fingerprint images and implementing a better feature extraction algorithm.

6 Conclusions and Future Work

We have proposed a novel fingerprint matching algorithm which operates in two stages: registration of the template and input fingerprint images and minutiae matching. The primary advantage of our algorithm is the accurate registration result. Registration between two fingerprints is achieved through maximization of mutual information, which is estimated from orientation field. This method is much more similar to the human behavior when comparing two fingerprints. As a result, the errors of misalignment, which often happens in a minutiae-based registration, dramatically decreased. A hierarchy registration approach is designed to speed up the registration. In addition, the mutual information acquired in the registration stage is incorporated into the final decision of matching result. In minutiae matching, we propose a fuzzy approach to the computation of matching scores. The matching result of two minutiae is given by a similarity level ranging from 0 to 1 that indicates how exactness they are matched, which gives a better result than the simple "matched" or "unmatched". Finally, all the similarity levels are averaged to get the statistical result. The average similarity level together with mutual information and the number of matched minutiae gives the matching score. Experimental results show that our algorithm can reliably find the accurate registration and achieves excellent verification performance.

Based on the experimental results, we find out that registration errors mainly result from too little area of overlapped sections'. This is not serious because when overlapped area becomes too little, there will be no sufficient evidence to verify the matching result. Another work needs to be done in future is to tackle the problem of searching parameter space as the size of fingerprint and the degree of rotation increases. A good optimization algorithm may address this issue. Most of matching errors are induced by the nonlinear deformation and poor quality images. Due to the presence of such a deformation, the elastic matching box must be large enough to tolerate it, which may increase the possibility of false matching. We need to design better fingerprint enhancement and minutiae extraction algorithms.

Acknowledgements

This work was partially supported by Hundred Talents Programs of the Chinese Academy of Sciences, the Natural Science Foundation of China, Grant No. 60172056 and 697908001, and Watchdata Digital Company. We would like to give our grates to the Universit? di Bologna of Italy because of the fingerprint database for testing our algorithm. We also thank our colleagues for devoted discussion about our work.

References

[1] R. Bahuguna, “Fingerprint Verification Using Hologram Matched Filterings,” *Proc. Biometric Consortium Eighth Meeting*, San Jose, California, June 1996.

[2] Y. S. Chen and W.H. Hsu, “A Modified Fast Parallel Algorithm for Thinning Digital Patterns,” *Pattern Recognition Letters*, vol. 7, no. 2, pp.99-106, 1988.

[3] A. Farina, Z.M. Kov?cs-Vajna, and A. Leone, “Fingerprint Minutiae Extraction from Skeletonized Binary Images,” *Pattern Recognition*, vol.32, no. 5, 1999, 877-889.

[4] S. Gold and A. Rangarajan, “A Graduated Assignment Algorithm for Graph Matching,” *IEEE Trans. Pattern Analysis and Machine Intelligence*, Vol.18, No.4, pp.377-388, 1996.

[5] R.M. Haralick, L.T. Watson, and T.J. Laffey, “The Topographic Primal Sketch,” *Int. J. Robotics Research*, vol. 2, pp. 50-72, 1983.

[6] D.K. Isenor and S.G. Zaky, “Fingerprint Identification Using Graph Matching,” *Pattern Recognition*, Vol. 19. No.2, 1986.

[7] A. Jain, L. Hong, and R. Bolle, “On-line Fingerprint Verification,” *IEEE Trans. Pattern Analysis and Machine Intelligence*, Vol.19, No. 4, pp.302-314, 1997.

[8] A.K. Jain, L. Hong, S. Pankanti, and R. Bolle, “An Identity Authentication System Using Fingerprints,” *Proc. IEEE*, Vol.85, pp.1365-1388, Sep. 1997.

[9] A.K. Jain, S. Prabhakar, S. Chen, “Combination Multiple Matchers for a High Security Fingerprint Verification System”, *Pattern Recognition Letters*, Vol.20, pp.1371-1379, 1999.

[10] A.K. Jain, S. Prabhakar, L. Hong, and S. Pankanti, “Filterbank-Based Fingerprint Matching,” *IEEE Trans. Image Processing*, Vol.9, No.5, pp. 846-859, 2000.

[11] X. Jiang, W. Yau, “Fingerprint Minutiae Matching Based on the Local and Global Structures”, *International Conference on Pattern Recognition*, pp. 1038-1041, Spain, 2000.

[12] Z.M. Kov?cs -Vajna, “A Fingerprint Verification System Based on Triangular Matching and Dynamic Time Warping,” *IEEE Trans. Pattern Analysis and Machine Intelligence*, Vol. 22, No.11, pp. 1266-1276, 2000.

[13] H.C. Lee and R.E. Gaensslen, eds., *Advances in Fingerprint Technology*, New York: Elsevier, 1991.

[14] D. Maio, D. Maltoni, “Direct Gray-scale Minutiae Detection in Fingerprints,” *IEEE Trans. Pattern Analysis and Machine Intelligence*, Vol.19, No.1, pp.27-38, 1997.

[15] A. Ranade and A. Rosenfeld, “Point Pattern Matching by Relaxation,” *Pattern Recognition*, Vol.12, No.2, pp.269-275, 1993.

[16] A.R. Rao, *A Taxonomy for Texture Description and Identification*, New York: Springer-Verlag, 1990.

[17] N. Ratha, K. Karu, S. Chen, and A. K. Jain, “A Real-Time Matching System for Large Fingerprint Databases,” *IEEE Trans. Pattern Analysis and Machine Intelligence*, Vol.18, No.8, pp. 799-813, 1996.

[18] J.P.P. Starink and E. Backer, “Finding Point Correspondence Using Simulated Annealing,” *Pattern Recognition*, vol.28, no.2, pp.231-240, 1995.

[19] M. Tico and P. Kuosmanen, “A Topographic Method for Fingerprint Segmentation,” *Proceedings on the 6th International Conference on Image Processing*, vol. 1, pp.36-40, Kobe, Japan, October 1999.

[20] J. Ton and A.K. Jain, “Registering Landset Images by Point Matching,” *IEEE Trans. Geoscience and Remote Sensing*, vol.27, no.5, pp.642-651, 1989.

[21] P. Viola, *Alignment By Maximization of Mutual Information*, Ph. D thesis, M.I.T. Artificial Intelligence Laboratory, 1995.

[22] J. Yang, L. Liu and T. Jiang, “An Improved Method for Extraction of Fingerprint Features,” *Proc. International Conference on Image and Graph*, August 2002, Anhui, China.

Table Captions

Table 1. Statistics of MI and errors of registrations.

Table 2. FAR and FRR with different threshold values ($W = 8$, $n = 18$, $T_s = 2.0$, $T_d = 1.2$).

Table 1. Statistics of MI and errors of registrations

Algorithm	Parameters	Mean		Standard Deviation		Errors of Registration
		Same	Different	Same	Different	
Proposed	$W = 8, n = 9$	1.4135	0.9528	0.1865	0.1515	6
	$W = 8, n = 18$	1.8492	1.3162	0.2192	0.1544	9
	$W = 8, n = 36$	2.2930	1.7773	0.2292	0.1366	50
Minutiae-based	——					59

Table 2. FAR and FRR with different threshold values ($W = 8$, $n = 18$, $T_s = 2.0$, $T_d = 1.2$).

Threshold Value	FAR	FRR
15	0%	12.5%
14	0.00744%	11.99%
13	0.04092%	11.05%
12	0.08185%	10.12%
11	0.19717%	9.69%
10	0.43155%	9.18%

Figure Captions

Fig. 1. Ridge bifurcation and ridge endpoint (a) bifurcation (b) endpoint.

Fig. 2. Fingerprint image and its mean directions in different blocks. The size of each block is 8? 8.

Fig. 3. Computation of input direction features.

Fig. 4. Estimation of joint distribution.

Fig. 5. Graphic representation of search space.

Fig. 6. Fingerprint images of different quality.

Fig. 7. Normalized distributions of MI for same fingers and different fingers (W=8, n=18).

Fig. 8. Some registration results using our algorithm and minutiae-based algorithm. (1) template images (2) input images (3) registration results of proposed method (4) registration results of minutiae-based method.

Fig. 9. Registration result which is similar to human' comparison. (1) template image (2) input image (3) superposed gray-scale image. (4) superposed thinning image.

Fig. 10. Normalized matching scores distributions for same fingers and different fingers. (W=8, n=18).

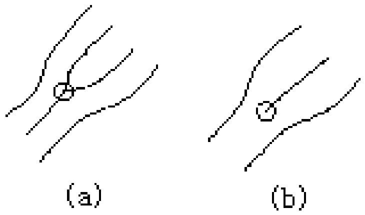

Fig. 1. Ridge bifurcation and ridge endpoint (a) bifurcation (b) endpoint.

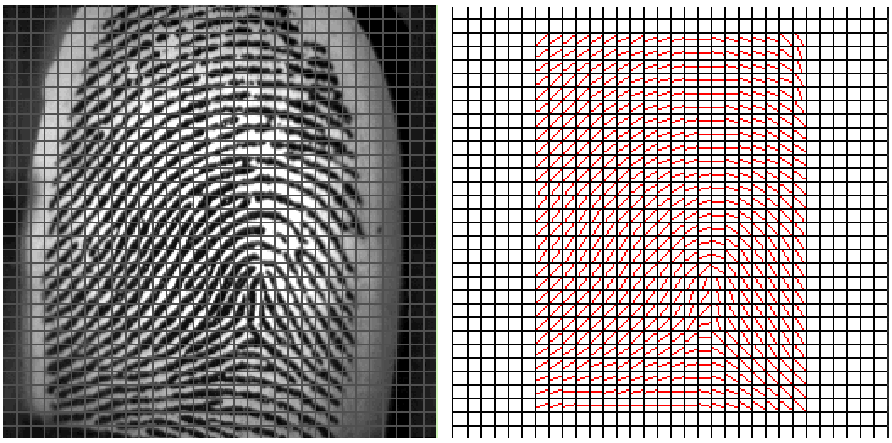

Fig. 2. Fingerprint image and its mean directions in different blocks. The size of each block is 8 ? 8.

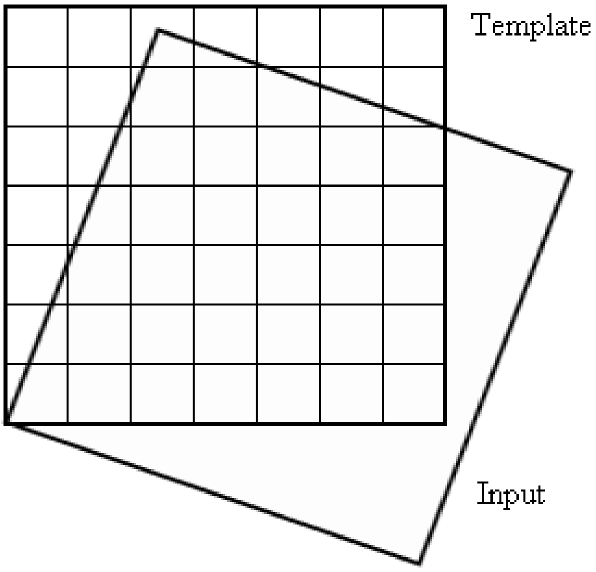

Fig. 3. Computation of input direction features.

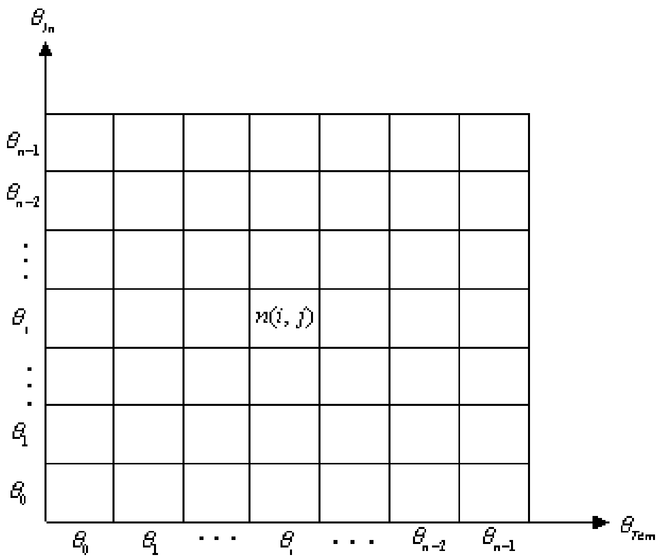

Fig. 4. Estimation of joint distribution.

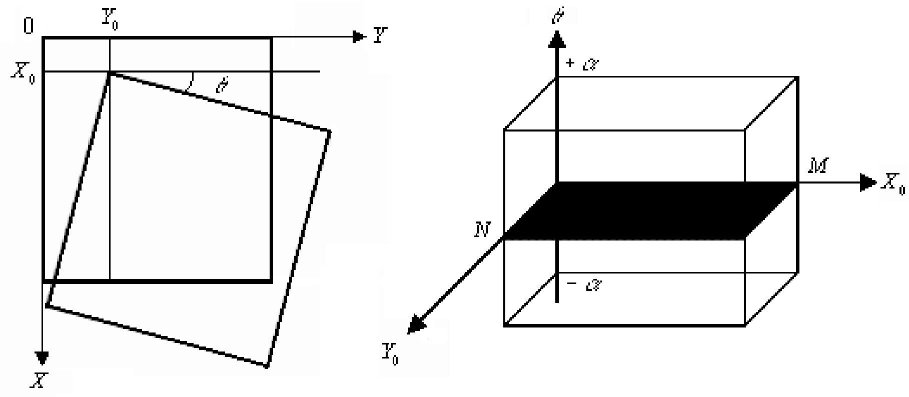

Fig. 5. Graphic representation of search space.

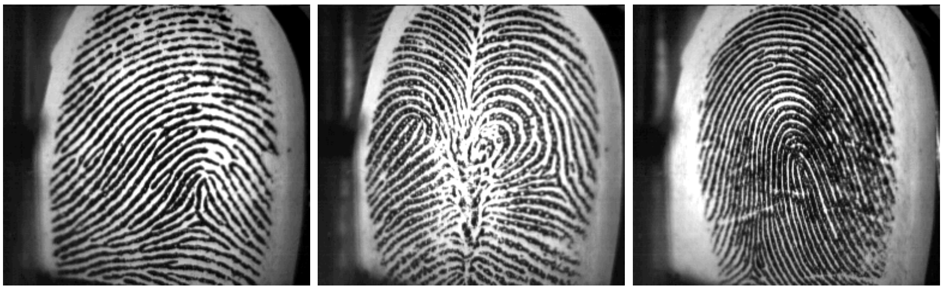

Fig. 6. Fingerprint images of different quality.

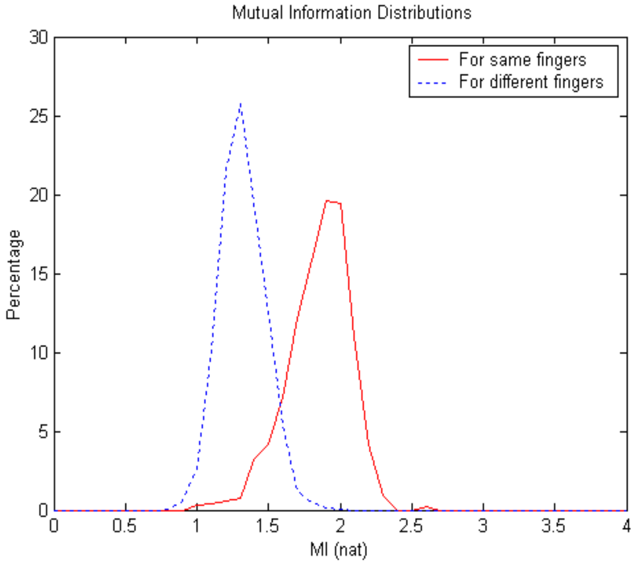

Fig. 7. Normalized distributions of MI for same fingers and different fingers (*W*=8, *n*=18).

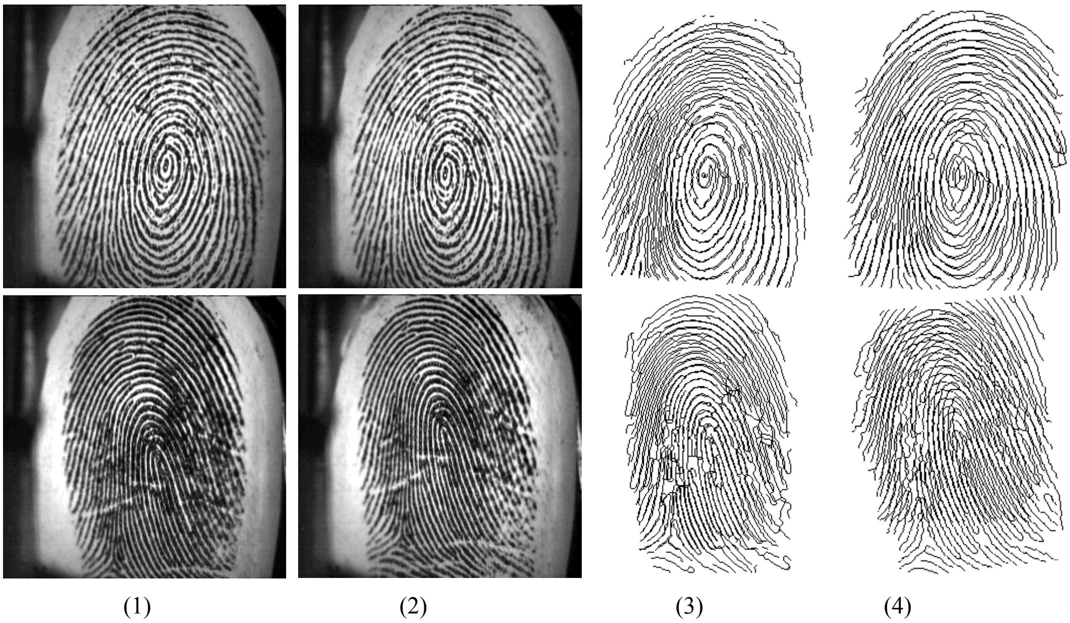

Fig. 8. Some registration results using our algorithm and minutiae-based algorithm. (1) template images (2) input images (3) registration results of proposed method (4) registration results of minutiae-based method.

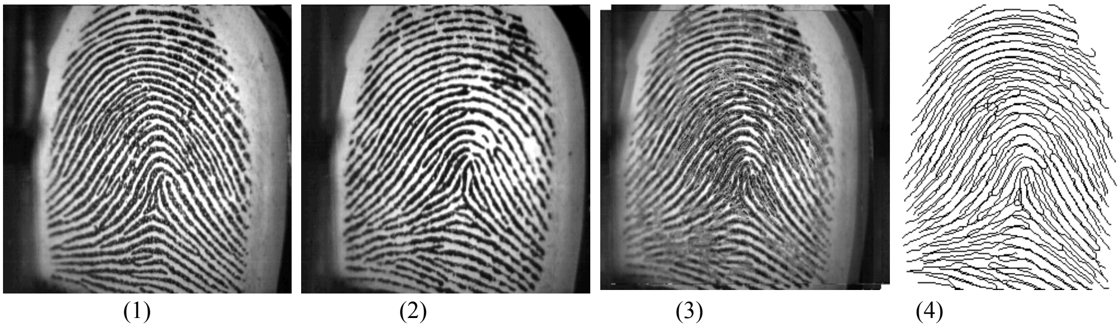

Fig. 9. Registration result which is similar to human' comparison. (1) template image (2) input image (3) superposed gray-scale image. (4) superposed thinning image.

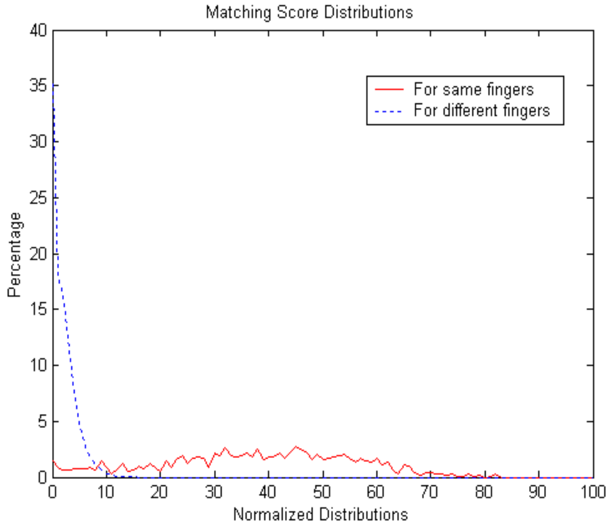

Fig. 10. Normalized matching scores distributions for same fingers and different fingers. (*W*=8, *n*=18).